# Mössbauer Spectroscopic Investigations of Metal Incorporation within Nasicon-related $NbTiP_3O_{12}$ †

**Frank J. Berry,*[a] Ramon Gancedo,[b] José F. Marco[b] and Robert C. Thied[a]**

[a] *Department of Chemistry, The Open University, Walton Hall, Milton Keynes MK7 6AA, UK*

[b] *Instituto de Quimica Fisica 'Rocasolano', Consejo Superior de Investigaciones Cientificas, Serrano 119, 28006 Madrid, Spain*

The reaction of Nasicon-related $NbTiP_3O_{12}$ (Nasicon = $Na_3Zr_2Si_2PO_{12}$) with elemental iron to give materials of composition $Fe_xNbTiP_3O_{12}$ ($0.00 < x \leqslant 0.33$) resulted in the incorporation of $Fe^{2+}$ in a distribution of similar environments within the type I octahedral interstitial sites. The decidedly positive $^{57}Fe$ Mössbauer chemical isomer shifts are associated with the longer distances between the highly ionic $Fe^{2+}$ species and the oxygen atoms which define the interstitial sites. Heating of the materials in air induced the migration of $Fe^{2+}$ from the type I sites to the surface where they were oxidised and formed a macroscopic iron(III) oxide phase. The reaction of $NbTiP_3O_{12}$ with elemental tin to give materials of composition $Sn_xNbTiP_3O_{12}$ ($0.00 < x \leqslant 0.50$) also resulted in the accommodation of $Sn^{2+}$ within the type I sites. The highly positive $Sn^{2+}$ Mössbauer chemical isomer shifts are interpreted in terms of the presence of highly ionic $Sn^{2+}$ species. Thermal treatment in air induced the migration of the $Sn^{2+}$ ions from the type I sites to the surface where they were oxidised to a discrete tin(IV) oxide phase. Compounds of composition $Fe_{0.25-x}Sn_xNbTiP_3O_{12}$ ($0.00 \leqslant x \leqslant 0.25$) have been prepared and the $Fe^{2+}$ and $Sn^{2+}$ ions found to occupy the same sites as in $Fe_xNbTiP_3O_{12}$ and $Sn_xNbTiP_3O_{12}$.

Compounds of composition $A^IM^{IV}{}_2P_3O_{12}$ have structures which involve the corner sharing of $PO_4$ tetrahedra with $MO_6$ octahedra thereby producing a three-dimensional linked channel network in which the A ions can be located.[1-4] The A ions can occupy two different types of sites within the channels.[3] The type I sites have a distorted octahedral co-ordination and are situated between two $MO_6$ octahedra along the *c* axis to produce ribbons of $O_3MO_3AO_3MO_3$. The type II sites are larger with eight to ten co-ordinating oxygen ions and are located between the ribbons. The structure is amenable to substitution on the A, M or phosphorus sites and a wide range of isostructural materials can be formed. The occupancy of the types I and II sites can also be varied from four to zero. For example, the compound $Na_3Zr_2Si_2PO_{12}$, Nasicon, has sodium ions in both types I and II sites and has attracted considerable interest because of its high sodium-ion mobility.[1,2]

The white compound of composition $NbTiP_3O_{12}$ with vacant types I and II sites also adopts the Nasicon-type structure and has been shown to be capable of direct reaction with several electropositive metals to give blue-black solids in which the metallic species are envisaged as being incorporated within the vacant sites.[5] We have recently shown[6] that the reaction of $NbTiP_3O_{12}$ with elemental iron and tin to give compounds of the type $Fe_{0.33}NbTiP_3O_{12}$ and $Sn_{0.5}NbTiP_3O_{12}$ involves the incorporation of $Fe^{2+}$ and $Sn^{2+}$ within the octahedral type I sites of the $NbTiP_3O_{12}$ structure. In this paper we report on the examination of these materials by transmission-mode $^{57}Fe$- and $^{119}Sn$-Mössbauer spectroscopy to examine the location of the divalent metallic species incorporated within the channels, and also by conversion electron Mössbauer spectroscopy to examine the nature of the tin and iron in the surface layers of the solids. The effect on the incorporated iron and tin of heating in air has also been investigated.

## Experimental

The compound $NbTiP_3O_{12}$ was prepared by the sequential heating of a stoichiometric mixture of niobium(V) oxide, titanium(IV) oxide (Anatase) and ammonium dihydrogen phosphate in air at 200 (12), 600 (6), 900 (15), 1000 (5) and finally at 1300 °C (4 h). Iron and tin were incorporated into $NbTiP_3O_{12}$ to give materials of composition $Fe_xNbTiP_3O_{12}$ ($0.00 < x \leqslant 1.00$), $Sn_xNbTiP_3O_{12}$ ($0.00 < x \leqslant 1.00$) and $Fe_{0.25-x}Sn_xNbTiP_3O_{12}$ ($0.00 \leqslant x \leqslant 0.25$) by heating $NbTiP_3O_{12}$ with the appropriate powdered elemental metals, or with mixtures of metals, at 900 °C (24 h) in evacuated sealed quartz tubes. Compounds of composition $Fe_{0.25-x}Sn_xNbTiP_3O_{12}$ ($0.00 \leqslant x \leqslant 0.25$) were also prepared by heating $Fe_{0.25}NbTiP_3O_{12}$ or $Sn_xNbTiP_3O_{12}$ with the appropriate amounts of powdered elemental tin or iron at 900 °C (24 h) in evacuated sealed quartz tubes. Samples of $Fe_{0.33}NbTiP_3O_{12}$ and $Sn_{0.50}NbTiP_3O_{12}$ were subsequently heated in air at temperatures between 50 and 1000 °C (12 h).

Mössbauer spectra were recorded with a microprocessor-controlled Mössbauer spectrometer using $^{57}Co$–Rh and $Ca^{119m}SnO_3$ sources. The drive velocity was calibrated with a $^{57}Co$–Rh source and a natural iron foil. All the $^{57}Fe$ Mössbauer spectra were computer fitted by constraining the areas of the peaks representing each doublet to be equal and with all peaks of equal linewidth. The $^{57}Fe$ Mössbauer isomer shifts are referred to α-iron and the $^{119}Sn$ Mössbauer isomer shifts to tin(IV) oxide. Conversion electron Mössbauer spectroscopy (CEMS) was performed with a parallel-plate avalanche counter filled with acetone at a pressure of *ca.* 60 Torr (≈7980 Pa). The samples were suspended in acetone and then transferred to the conducting berylium counter cathode where, on evaporation of the acetone, they formed a thin and even layer.

X-Ray powder diffraction data were recorded with a Siemens D5000 diffractometer using Cu-Kα radiation.

Titanium K-edge XANES (X-ray absorption near-edge structure) spectra were recorded at the Daresbury Synchrotron Radiation Source operating at an energy of 2.0 GeV and an average current of 200 mA at station 7.1 (titanium K-edge, 4965 eV).

† *Non-SI unit employed:* eV ≈ $1.60 \times 10^{-19}$ J.

## Results and Discussion

*Compounds of Composition* $Fe_{0.33}NbTiP_3O_{12}$.—The reaction of white $NbTiP_3O_{12}$ with elemental iron gave blue-black powders, $Fe_xNbTiP_3O_{12}$. Materials in which $x \leqslant 0.33$ were shown by X-ray powder diffraction to be similar to those previously obtained.[6] The variation of the lattice parameters with increasing iron content is shown in Table 1. Materials prepared from reactants in which the iron content exceeded 0.33 were found by X-ray powder diffraction to be multiphasic and contained iron phosphate phases which precluded rigorous interpretation of the diffraction data.

The transmission-mode $^{57}Fe$ Mössbauer spectrum recorded at 298 K from the material of composition $Fe_{0.33}NbTiP_3O_{12}$ (Fig. 1) was best fitted to five partially superimposed absorptions designated as A–E. The $^{57}Fe$ Mössbauer parameters are collected in Table 2.

The spectrum is dominated by the $Fe^{2+}$ components C–E which amount to *ca.* 90% of the total area of the spectrum. Our previous structural study[6] by analysis of the X-ray powder diffraction data using the Rietveld method showed that the incorporated iron is located only in the octahedral type I sites. The $^{57}Fe$ Mössbauer spectrum shows that iron is predominantly incorporated as $Fe^{2+}$ over a distribution of approximately octahedral sites. We associate the adoption by $Fe^{2+}$ of a distribution of octahedrally co-ordinated oxygen sites with the reduction of $Nb^{5+}$ or $Ti^{4+}$ in $NbTiP_3O_{12}$ by electrons generated during the incorporation of elemental iron as $Fe^{2+}$. The features observed in the titanium K-edge XANES spectra (Fig. 2) recorded from $NbTiP_3O_{12}$ and $Fe_{0.33}NbTiP_3O_{12}$ (which have been labelled $A_1$, $A_2$, B, C, $D_1$, $D_2$ according to the literature[7–9]) occurred at identical energies in both materials and are similar to those reported[7–11] for $Ti^{4+}$. Since the presence of $Ti^{3+}$ would cause a shift in the XANES values to lower energies[11] the results suggest that the incorporation of iron as $Fe^{2+}$ into $NbTiP_3O_{12}$ is accompanied by some reduction of $Nb^{5+}$ to $Nb^{4+}$. The consequence appears to be that the type I octahedral sites in $NbTiP_3O_{12}$ are trigonally elongated along [001] and share faces perpendicular to [001] with either $NbO_6$ or $TiO_6$ octahedra in which the cations may be $Nb^{5+}$, $Nb^{4+}$ or $Ti^{4+}$. The presence of combinations of these cations of different charge appears to cause the displacement of the $Fe^{2+}$ ions from regular octahedral oxygen co-ordination and is reflected by components C–E in the $^{57}Fe$ Mössbauer spectrum. The result is consistent with the high thermal parameter for iron deduced by analysis of the X-ray powder diffraction data.[6] The Δ (quadrupole splitting) value of the C site is similar to the Δ values observed in $(Mg,Fe)_3(PO_4)_2$,[12] while the Δ values of the D and E sites are significantly smaller. It is known[13] that an increased distortion of the co-ordination polyhedra around a divalent iron species will increase the lattice contribution to the electric-field gradient and give smaller quadrupole splittings. Hence the smaller Δ values of the D and E components as compared to the C component may reflect more distortion around the $Fe^{2+}$ species contributing to the D and E components of the spectrum. This distortion may be related to the presence of different Nb–Ti configurations, in different oxidation states, around the $Fe^{2+}$ sites in the $Fe_{0.33}NbTiP_3O_{12}$ structure. Component B of the Mössbauer spectrum is characteristic of $Fe^{3+}$ and may be associated with a small amount of oxidised iron at the surface of the host lattice (see below). The component A is characterised by a large quadrupole splitting and we associate this with the presence of a small amount (*ca.* 5%) of $Fe^{2+}$ in the type II sites or in an impurity phase which is also undetected by X-ray powder diffraction.

The highly positive $^{57}Fe$ Mössbauer chemical isomer shifts for the $Fe^{2+}$ species[14a,15] in $Fe_{0.33}NbTiP_3O_{12}$ may be associated with the average iron–oxygen distances[6] of 2.376 Å. These distances are about 0.2 Å longer than normally found for $Fe^{2+}$ when octahedrally co-ordinated to oxygen[16] and we envisage the presence of $Fe^{2+}$ species which are highly ionic in character and which interact only weakly with the surrounding oxygen atoms.

**Table 1** Lattice parameters recorded from materials of composition $Fe_xNbTiP_3O_{12}$

| | $a = b$ (±0.02)/Å | $c$ (±0.03)/Å |
|---|---|---|
| $NbTiP_3O_{12}$ | 8.56 | 21.98 |
| $Fe_{0.15}NbTiP_3O_{12}$ | 8.60 | 21.78 |
| $Fe_{0.25}NbTiP_3O_{12}$ | 8.61 | 21.51 |
| $Fe_{0.33}NbTiP_3O_{12}$ | 8.61 | 21.45 |

**Table 2** Iron-57 Mössbauer parameters recorded from $Fe_{0.33}NbTiP_3O_{12}$ at various temperatures

| $T$/K | Site | $\delta$[a]/mm s$^{-1}$ | $\Delta$[a]/mm s$^{-1}$ | $\Gamma$/mm s$^{-1}$ | Area (%) |
|---|---|---|---|---|---|
| 298 | A | 1.23 | 2.21 | 0.35 | 4 |
| | B | 0.38 | 1.03[b] | 0.35 | 5 |
| | C | 1.28 | 1.44 | 0.35 | 16 |
| | D | 1.31 | 1.03 | 0.35 | 36 |
| | E | 1.32 | 0.65 | 0.35 | 38 |
| 199 | A | 1.34 | 2.25 | 0.37 | 6 |
| | B | 0.39 | 1.03[b] | 0.37 | 6 |
| | C | 1.37 | 1.65 | 0.37 | 19 |
| | D | 1.38 | 1.19 | 0.37 | 34 |
| | E | 1.40 | 0.78 | 0.37 | 34 |
| 148 | A | 1.30 | 2.50 | 0.39 | 5 |
| | B | 0.40[b] | 1.03[b] | 0.39 | 5 |
| | C | 1.40 | 1.91 | 0.39 | 18 |
| | D | 1.41 | 1.38 | 0.39 | 35 |
| | E | 1.42 | 0.91 | 0.39 | 37 |
| 124 | A | 1.30 | 2.51 | 0.41 | 5 |
| | B | 0.40[b] | 1.03[b] | 0.41 | 5 |
| | C | 1.42 | 1.96 | 0.41 | 20 |
| | D | 1.43 | 1.43 | 0.41 | 36 |
| | E | 1.43 | 0.96 | 0.41 | 34 |
| 100 | A | 1.30 | 2.69 | 0.41 | 4 |
| | B | 0.40[b] | 1.03[b] | 0.41 | 4 |
| | C | 1.44 | 2.08 | 0.41 | 21 |
| | D | 1.45 | 1.59 | 0.41 | 37 |
| | E | 1.45 | 1.09 | 0.41 | 34 |
| 77 | A | 1.29 | 3.42 | 0.41 | 3 |
| | B | 0.40[b] | 1.03[b] | 0.41 | 3 |
| | C | 1.46 | 2.18 | 0.41 | 25 |
| | D | 1.47 | 1.71 | 0.41 | 43 |
| | E | 1.46 | 1.22 | 0.41 | 26 |
| 50 | A | 1.22 | 3.41 | 0.36 | 2 |
| | B | 0.40[b] | 1.03[b] | 0.36 | 2 |
| | C | 1.47 | 2.28 | 0.36 | 28 |
| | D | 1.49 | 1.92 | 0.36 | 46 |
| | E | 1.46 | 1.55 | 0.36 | 22 |
| 30 | A | 1.29 | 3.42 | 0.33 | 2 |
| | B | 0.40[b] | 1.03[b] | 0.33 | 2 |
| | C | 1.48 | 2.34 | 0.33 | 28 |
| | D | 1.49 | 2.00 | 0.33 | 46 |
| | E | 1.47 | 1.69 | 0.33 | 21 |
| 15 | A | 1.29 | 3.42 | 0.33 | 2 |
| | B | 0.40[b] | 1.03[b] | 0.33 | 2 |
| | C | 1.47 | 2.36 | 0.33 | 25 |
| | D | 1.49 | 2.04 | 0.33 | 44 |
| | E | 1.47 | 1.77 | 0.33 | 27 |

[a] The average errors in the Mössbauer parameters of site A are estimated to be ±0.08 mm s$^{-1}$, and ±0.03 mm s$^{-1}$ in the other sites. [b] Fixed parameter in the fitting procedure.

The spectra recorded between 199 and 15 K (Fig. 1) also showed five absorptions. The spectra recorded between 148 and 77 K were of similar shape but the two peaks enveloping the various components were broader than those recorded at higher or lower temperatures. In order to determine the changes occurring in the major components of the spectra, *i.e.* absorptions C–E, the following fitting procedure was adopted.

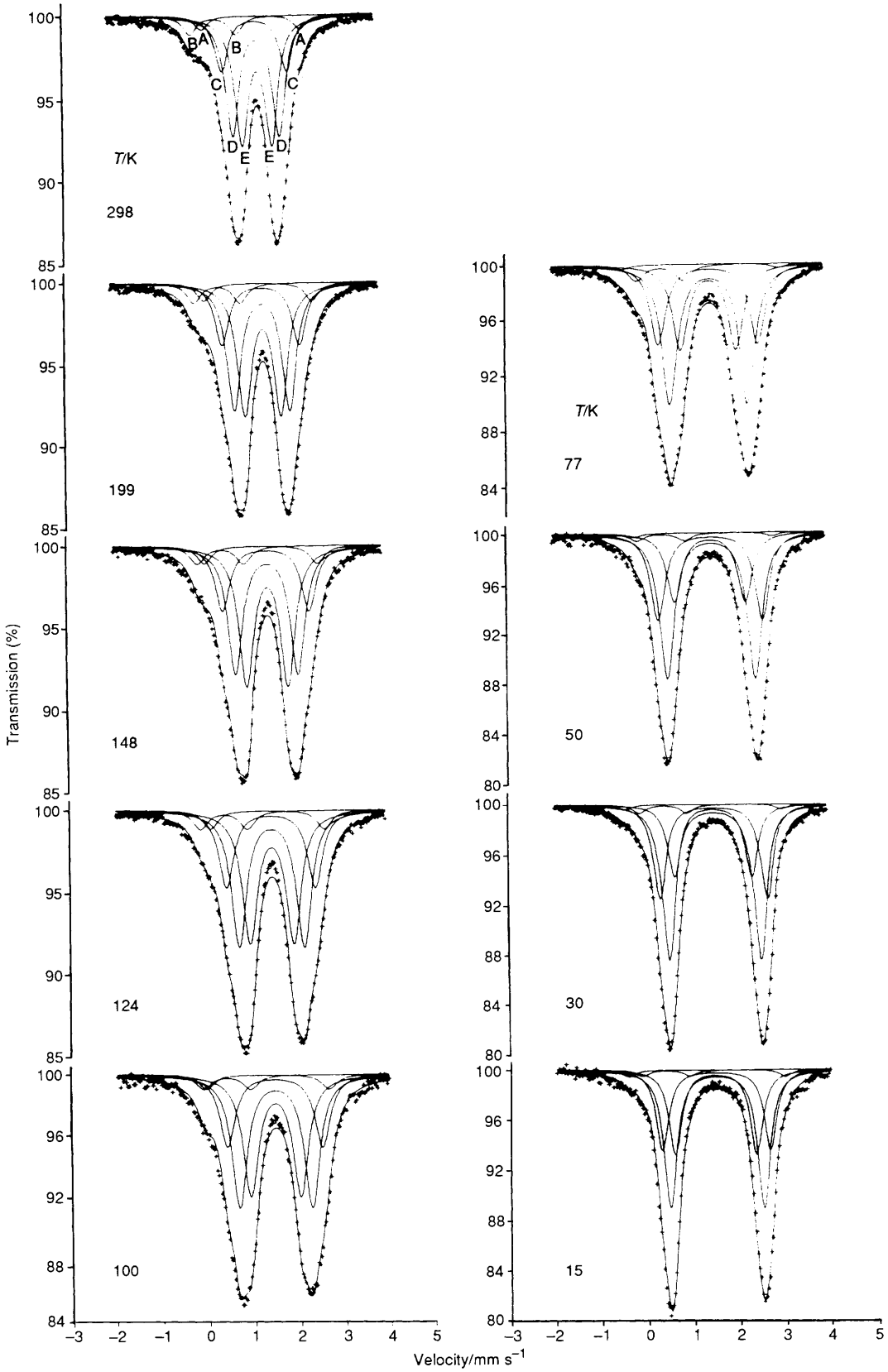


**Fig. 1** Transmission-mode $^{57}$Fe Mössbauer spectra recorded from $Fe_{0.33}NbTiP_3O_{12}$ at 15–298 K

Since the quadrupole splitting of the minor high-spin $Fe^{3+}$ species B is not expected to change with decreasing temperature, it was constrained to the same value in all the spectra recorded at different temperatures. This value was obtained from the fitting of the CEM spectrum in which the B species shows an enhanced intensity (see below). The chemical isomer shift of the $Fe^{3+}$ absorption was constrained to the value obtained from the spectrum recorded at 15 K. The intensity of the minor $Fe^{3+}$ component B in spectra recorded at temperatures lower than 298 K was constrained to be equal to that of the minor $Fe^{2+}$

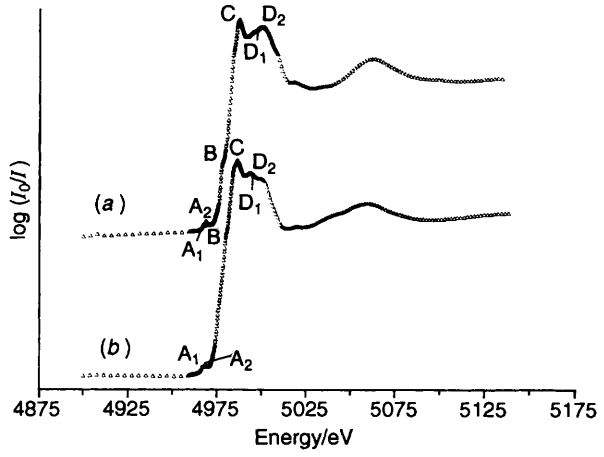


**Fig. 2** Titanium K-edge XANES spectra of (*a*) $NbTiP_3O_{12}$ and (*b*) $Fe_{0.33}NbTiP_3O_{12}$

component A which has a comparable intensity at 298 K. The imposition of these constraints, although mitigating against the accurate identification of the Mössbauer parameters of the minor $Fe^{2+}$ component A, enabled more facile computation of the more dominant $Fe^{2+}$ components C–E.

The values of the quadrupole splitting data for the $Fe^{2+}$ components C–E increase with decreasing temperature according to the trends described in Table 2 and Fig. 3 and as expected for high-spin $Fe^{2+}$ species.[17] The quadrupole splitting is the net result of the lattice and valence contributions to the electric-field gradient. In the case of $Fe^{2+}$ the valence contribution is the dominant contribution and as the temperature decreases the valence contribution to the electric-field gradient increases[13] bringing about an increase in the values of Δ.

The chemical isomer shifts (δ) for components C–E increase with decreasing temperature as shown in Fig. 4 and Table 2. The trend is a reflection of the second-order Doppler shift, indeed the observed linear dependence of δ between 77 and 298 K gives a slope ($7.9 \times 10^{-4}$, $7.2 \times 10^{-4}$ and $6.2 \times 10^{-4}$ mm $s^{-1}$ $K^{-1}$ for the C, D and E components, respectively) which compares well with the hypothetical value of $7.32 \times 10^{-4}$ mm $s^{-1}$ $K^{-1}$ which corresponds to the high-temperature limit of the Einstein model.[18]

The CEM spectrum recorded from $Fe_{0.33}NbTiP_3O_{12}$ is shown in Fig. 5. The data were best fitted to components similar to those identified in the transmission-mode spectrum. However, the intensity of the quadrupole split absorption B, $\delta = 0.39$ mm $s^{-1}$, $\Delta = 1.03$ mm $s^{-1}$, corresponding to the presence of $Fe^{3+}$, was greatly enhanced (17% in the CEMS as compared with 5% in the transmission-mode spectrum). Given that the data recorded by CEMS emanate from the top 300 nm of the material under examination,[19] the results suggest that the $Fe^{3+}$ component in $Fe_{0.33}NbTiP_3O_{12}$ is located in the surface layers. The decrease in the contribution of the $Fe^{2+}$ component C to the CEM spectrum as compared with that recorded in transmission geometry suggests that the $Fe^{3+}$ in the superficial layers is located within sites which contribute to the C spectral component and, presumably, arises from the atmospheric oxidation of $Fe^{2+}$.

Finally, we confirm that the $Fe^{2+}$ components of the $^{57}Fe$ Mössbauer spectra recorded from materials with iron contents less than 0.33 were similar to the data recorded from $Fe_{0.33}NbTiP_3O_{12}$.

*Heating of* $Fe_{0.33}NbTiP_3O_{12}$ *in air*. The variation in the lattice parameters of $Fe_{0.33}NbTiP_3O_{12}$ following treatment in air is shown in Table 3. The results show that thermal treatment in air at increasing temperatures gives materials with lattice parameters approaching those of $NbTiP_3O_{12}$. The X-ray

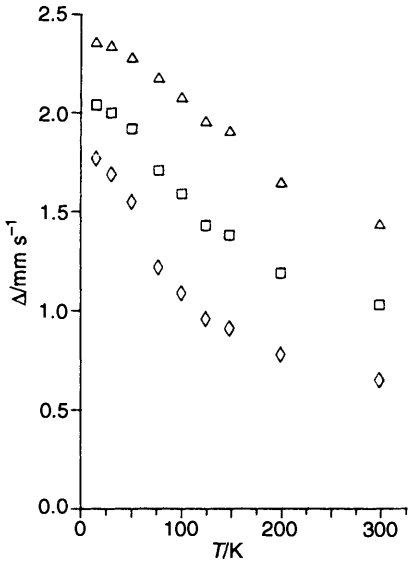


**Fig. 3** Variation in the quadrupole splitting (Δ) for the $Fe^{2+}$ components C (△), D (□) and E (◇) with temperature

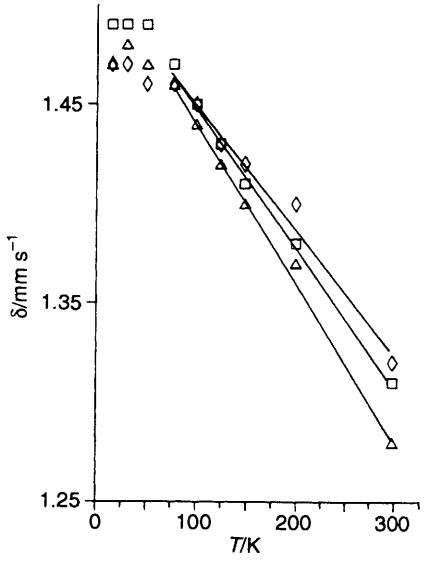


**Fig. 4** Variation in the chemical isomer shift (δ) for the $Fe^{2+}$ components C (△), D (□) and E (◇) with temperature

powder diffraction patterns also showed the $Fe_{0.33}NbTiP_3O_{12}$ to undergo partial degradation to $NbPO_5$ during the thermal treatment. The $^{57}Fe$ Mössbauer spectrum recorded from the material following treatment at 100 °C showed five absorptions similar to those observed in $Fe_{0.33}NbTiP_3O_{12}$ (see above). Subsequent heating at 200, 300 and 400 °C gave brown solids from which the Mössbauer spectra showed additional sextet patterns ($\delta = 0.38$ mm $s^{-1}$, $\Delta = -0.10$ mm $s^{-1}$; $H = 51.9$ T) characteristic[20] of $\alpha$-$Fe_2O_3$. Taken together the results suggest that thermal treatment in air induces the migration of $Fe^{2+}$ ions from the type I sites to the surface where they are oxidised to a macroscopic $\alpha$-$Fe_2O_3$ phase. The variation in the intensities of the three main Mössbauer spectral doublets corresponding to $Fe^{2+}$ as a function of heat treatment is depicted in Fig. 6. The results show that the migration of iron is almost complete when the materials are heated at 300 °C and is consistent with the variations in the lattice parameters (Table 3). The migration of $Fe^{2+}$ ions under moderate thermal conditions (200–300 °C) to the surface where they oxidise and form $\alpha$-$Fe_2O_3$ is consistent with the loosely bound nature of these species.

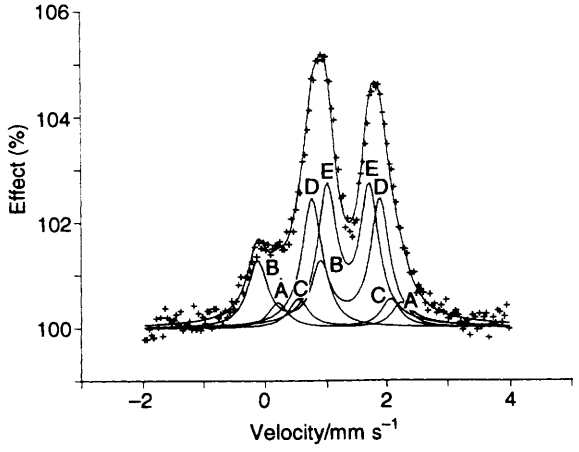


**Fig. 5** CEM spectrum recorded from $Fe_{0.33}NbTiP_3O_{12}$

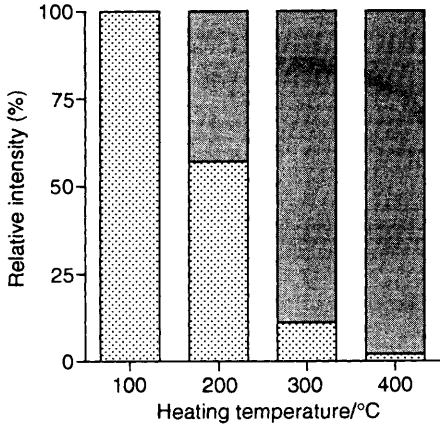


**Fig. 6** Variation in the spectral areas of $\alpha$-$Fe_2O_3$ (shaded) and $Fe^{2+}$ (dotted, *i.e.* the sum of the spectral areas of components C–E) within the $NbTiP_3O_{12}$ structure with heating temperature

*Compounds of Composition* $Sn_xNbTiP_3O_{12}$ ($0.00 < x \leqslant 1.00$).—The X-ray powder diffraction patterns recorded from the blue-black compounds of nominal composition $Sn_xNbTiP_3O_{12}$ ($0.00 < x \leqslant 1.00$) were similar to that previously recorded[6] from $Sn_{0.5}NbTiP_3O_{12}$. The *c* lattice parameter was found to increase with increasing tin content in the range $0.00 < x \leqslant 0.50$ whilst the *a* lattice parameter remained approximately constant (Table 4). The additional presence of metallic tin was observed in the X-ray powder diffraction patterns recorded from materials of nominal composition $Sn_{0.66}NbTiP_3O_{12}$ and $Sn_{1.00}NbTiP_3O_{12}$.

The transmission-mode $^{119}Sn$ Mössbauer spectra recorded at 298 K from materials in the composition range $0 < x \leqslant 0.50$ were all similar (Fig. 7) and best fitted to a quadrupole split absorption characteristic of $Sn^{2+}$, which we associate with tin in one site designated as the A site, together with a singlet of similar area and also characteristic of $Sn^{2+}$ which we associate with another site designated as the B site (Table 5). The possibility that the Mössbauer data could be interpreted in terms of two quadrupole split doublets with the large peak representing the superimposed high velocity components of the two species was examined. However, the need to apply additional constraints in order to achieve satisfactory convergence mitigated against the adoption of this model. The refinement of the X-ray powder diffraction data revealed[6] the $Sn^{2+}$ cations to be accommodated in the octahedral type I sites of the $NbTiP_3O_{12}$ structure with half of the centrally located species being displaced by *ca.* 0.3 Å along [001]. Hence the quadrupole split absorption may be associated with the distorted co-ordination of half the $Sn^{2+}$ species whilst the singlet component is indicative of the location of $Sn^{2+}$ in a regular octahedral site. The spectra recorded at 77 and 4.2 K were similar (Fig. 7). The displacement of only half the $Sn^{2+}$ ions may be associated with the structural properties of $NbTiP_3O_{12}$. It might be anticipated that $Sn^{2+}$ occupies a central location within the type I site when it is linked by the sharing of the faces perpendicular to [001] to only $TiO_6$ octahedra or to only $NbO_6$ octahedra. Statistically this would be expected to account for 50% of the type I sites. The remaining $Sn^{2+}$ in type I sites might be expected to be displaced from the central position when the site is linked to one $TiO_6$ octahedron and one $NbO_6$ octahedron.

**Table 3** Variation in lattice parameters of $Fe_{0.33}NbTiP_3O_{12}$ following heating in air

| *T*/°C | $a = b$ (±0.02)/Å | *c* (±0.03)/Å |
|---|---|---|
| 100 | 8.66 | 21.55 |
| 200 | 8.61 | 21.61 |
| 300 | 8.61 | 21.85 |
| 400 | 8.60 | 21.86 |
| 1000 | 8.61 | 22.05 |

**Table 4** Lattice parameters recorded from materials of composition $Sn_xNbTiP_3O_{12}$

| *x* | $a = b$ (±0.02)/Å | *c* (±0.03)/Å |
|---|---|---|
| 0.00 | 8.56 | 21.98 |
| 0.10 | 8.59 | 22.19 |
| 0.15 | 8.60 | 22.33 |
| 0.25 | 8.59 | 22.45 |
| 0.33 | 8.58 | 22.56 |
| 0.50 | 8.61 | 22.78 |
| 0.66 | 8.59 | 22.79 |
| 1.00 | 8.56 | 22.77 |

In such a situation the niobium or titanium ions adjacent to the Sn(A) sites would be expected to have slightly different atomic coordinates as compared to those linked to the Sn(B) sites. The higher Nb–Ti isotropic thermal parameter[6] in $Sn_{0.5}NbTiP_3O_{12}$ than in $NbTiP_3O_{12}$ supports such an interpretation. However, the accommodation of $Sn^{2+}$ in an undistorted site is unusual and suggests that the lone pair of electrons are primarily in the stereochemically inactive 5s orbital. This may be a reflection of the high cation repulsions which result from the rare location of this ion in a site which involves the face-sharing of octahedra containing very highly charged niobium and titanium cations.

It is notable that the $^{119}Sn$ Mössbauer chemical isomer shift data are more positive than those previously reported for $Sn^{2+}$ in oxygen co-ordination.[14b] The results are consistent with the refinement of the X-ray powder diffraction data[6] recorded from the compound $Sn_{0.5}NbTiP_3O_{12}$ which showed the octahedral tin atoms to be surrounded by six oxygen atoms at 2.62 Å and the remaining tin atoms to be co-ordinated by three oxygen atoms at 2.36 Å and three at 2.89 Å. Given that the four Sn–O bonds in SnO are 2.22 Å long,[21] the more positive $^{119}Sn$ Mössbauer chemical isomer shift data can be attributed to the higher co-ordination of $Sn^{2+}$ and the longer Sn–O distances in $Sn_{0.5}NbTiP_3O_{12}$. Such $Sn^{2+}$ species may be viewed as being highly ionic in character. The observed increase in spectral absorption at low temperature (Fig. 7) is indicative of a large difference in recoil-free fractions at 298 and 4.2 K and is consistent with the $Sn^{2+}$ species weakly interacting with its surrounding oxygen atoms at 298 K. The values of $\delta$ for both $Sn^{2+}$ species in the compounds $Sn_{0.25}NbTiP_3O_{12}$ and $Sn_{0.33}NbTiP_3O_{12}$ are especially interesting. Indeed, the $Sn^{2+}$ ion in the more regular of the two octahedral sites in these two low tin-containing materials has a chemical isomer shift approaching that predicted for an ideal stannous ion with a pure $5s^2$ electronic configuration.[22]

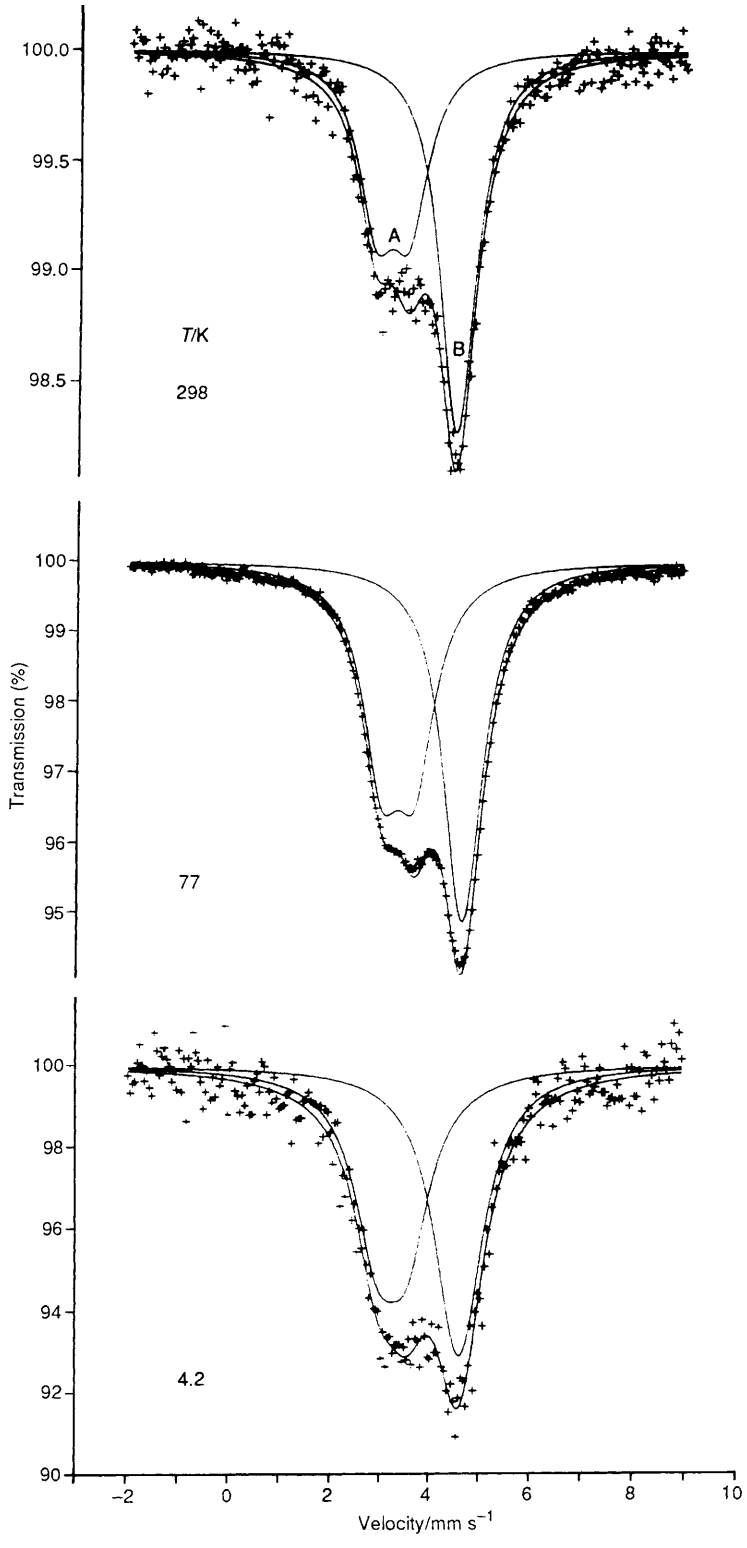


**Fig. 7** Tin-119 transmission Mössbauer spectra recorded from $Sn_{0.5}NbTiP_3O_{12}$ at different temperatures

The $^{119}Sn$ Mössbauer spectra recorded from the compounds $Sn_{0.66}NbTiP_3O_{12}$ and $Sn_{1.00}NbTiP_3O_{12}$ showed an additional single absorption, $\delta = 2.58$ mm s$^{-1}$, characteristic of metallic tin.[14c] The results are consistent with the X-ray powder diffraction data and indicate that the upper limit in the amount of tin which can be accommodated within the channels of the $NbTiP_3O_{12}$ structures is reached at *ca.* $x = 0.5$. Given the XANES data described above which indicate that $Nb^{5+}$ as opposed to $Ti^{4+}$ in $NbTiP_3O_{12}$ is reduced on the incorporation of metals as divalent cations, the material of composition $Sn_{0.5}NbTiP_3O_{12}$ corresponds to the situation where all the $Nb^{5+}$ has been reduced to the tetravalent form. It would appear that the resistance of $Ti^{4+}$ to reduction inhibits the incorporation of further amounts of tin.

Finally, we would comment that the CEM spectrum recorded from $Sn_{0.50}NbTiP_3O_{12}$ was identical to that obtained in transmission mode.

*Heating of* $Sn_{0.5}NbTiP_3O_{12}$ *in air*. The variation in the lattice

**Table 5** Tin-119 transmission-mode Mössbauer parameters recorded at 298 K from materials of nominal composition $Sn_xNbTiP_3O_{12}$

| $x$ | Site | $\delta$ (±0.05)/mm s$^{-1}$ | $\Delta$ (±0.05)/mm s$^{-1}$ | Area (%) |
|---|---|---|---|---|
| 0.25 | A | 3.44 | 0.68 | 46 |
| | B | 4.50 | | 54 |
| 0.33 | A | 3.49 | 0.65 | 47 |
| | B | 4.57 | | 53 |
| 0.50 | A | 3.12 | 0.66 | 45 |
| | B | 4.44 | | 55 |
| 0.66 | A | 3.18 | 0.61 | 38 |
| | B | 4.46 | | 50 |
| | M | 2.54 | | 12 |
| 1.00 | A | 3.16 | 0.71 | 28 |
| | B | 4.45 | | 39 |
| | M | 2.58 | | 33 |

**Table 6** Variation in lattice parameters of $Sn_{0.5}NbTiP_3O_{12}$ following heating in air

| $T$/°C | $a = b$ (±0.02)/Å | $c$ (±0.03)/Å |
|---|---|---|
| 50 | 8.57 | 22.75 |
| 100 | 8.57 | 22.73 |
| 350 | 8.60 | 22.80 |
| 400 | 8.61 | 22.84 |

**Table 7** Lattice parameters of compounds of type $Fe_{0.25-x}Sn_x$-$NbTiP_3O_{12}$

| Sample | $a = b$ (±0.02)/Å | $c$ (±0.03)/Å |
|---|---|---|
| $Fe_{0.05}Sn_{0.20}NbTiP_3O_{12}$ | 8.59 | 22.26 |
| $Fe_{0.10}Sn_{0.15}NbTiP_3O_{12}$ | 8.61 | 21.90 |
| $Fe_{0.15}Sn_{0.10}NbTiP_3O_{12}$ | 8.61 | 21.83 |
| $Fe_{0.20}Sn_{0.05}NbTiP_3O_{12}$ | 8.61 | 21.74 |

parameters of $Sn_{0.5}NbTiP_3O_{12}$ following thermal treatment in air is shown in Table 6. The results show that heating in air is accompanied by a change in lattice parameters towards those of $NbTiP_3O_{12}$. The X-ray powder diffraction patterns showed evidence of the partial degradation of $Sn_{0.5}NbTiP_3O_{12}$ to $NbPO_5$ and the formation of a tin(IV) oxide phase. The blue-black $Sn_{0.5}NbTiP_3O_{12}$ changed colour during the thermal treatment and, following heating at 1000 °C, became white. The $^{119}$Sn Mössbauer spectra recorded from materials heated in air at increasing temperatures showed the steady development of an absorption ($\delta$ 0.00 mm s$^{-1}$) characteristic of tin dioxide. The spectrum recorded from the material heated at 1000 °C showed only the single absorption characteristic of $SnO_2$. The variation in the spectral areas of the doublet and the singlet corresponding to $Sn^{2+}$ in $NbTiP_3O_{12}$ as a function of the thermal treatment is shown in Fig. 8. The formation of the tin dioxide phase on the surface was visible by scanning electron microscopy. As in the case of the iron-doped materials, the results are consistent with the presence of a potentially mobile $Sn^{2+}$ species within the channels of $NbTiP_3O_{12}$.

*Compounds of Composition* $Fe_{0.25-x}Sn_xNbTiP_3O_{12}$ ($0.00 \leqslant x \leqslant 0.25$).—The lattice parameters of compounds of the type $Fe_{0.25-x}Sn_xNbTiP_3O_{12}$ are collected in Table 7. The lattice parameters for a given composition were independent of whether iron and tin were incorporated within $NbTiP_3O_{12}$ simultaneously or by the reaction of iron with $Sn_xNbTiP_3O_{12}$ or of tin with $Fe_{0.25-x}NbTiP_3O_{12}$. Whilst the $a$ lattice parameter remained constant for all these compounds the $c$ lattice parameter varied linearly with composition as shown in Fig. 9. The results suggest that iron and tin occupy the same sites as in the compounds $Fe_xNbTiP_3O_{12}$ ($0.00 < x \leqslant 0.33$) and $Sn_xNbTiP_3O_{12}$ ($0.00 < x \leqslant 0.50$).

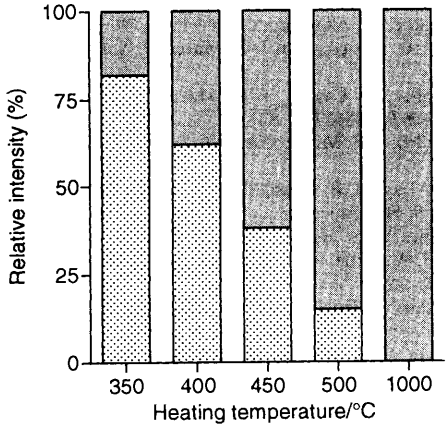


**Fig. 8** Variation in the Mössbauer spectral areas of $SnO_2$ (shaded) and $Sn^{2+}$ (dotted, *i.e.* the sum of the spectral areas of components A and B) within the $NbTiP_3O_{12}$ lattice with heating temperature

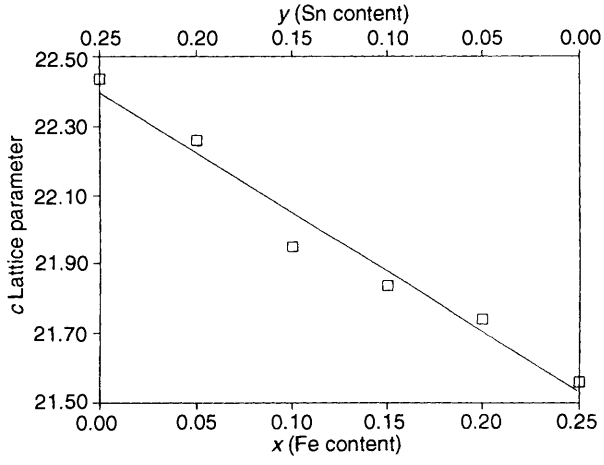


**Fig. 9** Variation in the $c$ lattice parameter of the compounds $Fe_{0.25-x}Sn_xNbTiP_3O_{12}$ with $x$. The straight line corresponds to the best linear fit

The $^{119}$Sn Mössbauer spectra recorded from these materials were identical to those obtained from the compounds $Sn_xNbTiP_3O_{12}$ ($0.00 < x \leqslant 0.50$) and show both the singlet and doublet components as described above. The $^{57}$Fe Mössbauer spectra showed the three absorptions C–E with parameters similar to those obtained from the compounds $Fe_xNbTiP_3O_{12}$ ($0 < x \leqslant 0.33$). The results indicate that there is no competition between tin and iron and that the $Fe^{2+}$ and $Sn^{2+}$ ions occupy the same locations as in iron- and tin-doped $NbTiP_3O_{12}$.

## Acknowledgements

We thank the Spanish Ministry of Education for the award of a Fellowship (to J. F. M.) and the British Council for travel grants (to R. G. and F. J. B.).

## References

1 P. Hagenmuller and W. van Gool (Editors), *Solid Electrolytes*, Academic Press, New York, 1978.
2 P. Vashista, J. N. Mundy and G. K. Shenoy (Editors), *Fast Ion Transport in Solids Electrodes and Electrolytes*, North Holland, New York, 1979.
3 L. O. Hagman and P. Kierkegaard, *Acta Chem. Scand.*, 1968, **22**, 1822.
4 R. Masse, A. Durif, J. C. Guitel and I. Tordjman, *Bull. Soc. Fr. Mineral. Cristallogr.*, 1972, **95**, 47.

5 G. V. Subba Rao, U. V. Varadaraju, K. A. Thomas and B. Sivasankar, *J. Solid State Chem.*, 1987, **70**, 101.
6 F. J. Berry, C. Greaves and J. F. Marco, *J. Solid State Chem.*, 1992, **96**, 408.
7 B. Poulmellec, F. Laguel, J. F. Marucco and B. Touzelin, *Phys. Status Solidi B*, 1986, **133**, 371.
8 B. Poulmellec, J. F. Marucco and B. Touzelin, *Phys. Status Solidi B*, 1986, **137**, 519.
9 F. Pichard-Lagnel, B. Poumellec and P. M. Cortes, *J. Phys. Chem. Solids*, 1989, **50**, 1211.
10 L. A. Grunes, *Phys. Rev. B*, 1983, **27**, 2111.
11 J. Wong, F. W. Lytle, R. P. Messmer and D. H. Maylotte, *Phys. Rev. B*, 1984, **30**, 5596.
12 H. Annersten, T. Ericsson and A. G. Nord, *J. Phys. Chem. Solids*, 1980, **41**, 1235.
13 R. Ingalls, in *An Introduction to Mössbauer Spectroscopy*, ed. L. May, Adam Hilger, London, 1971, p. 114.
14 N. N. Greenwood and T. C. Gibb, *Mössbauer Spectroscopy*, Chapman and Hall, London, 1971, (*a*) p. 112; (*b*) p. 388; (*c*) p. 418.
15 F. Menil, *J. Phys. Chem. Solids*, 1985, **46**, 763.
16 L. W. Finger, R. M. Hazen and T. Yogi, *Am. Mineral.*, 1979, **64**, 1002.
17 R. Ingalls, *Phys. Rev. A*, 1964, **133**, 787.
18 G. Amtahuer, H. Annersten and S. S. Hafner, *Z. Kristallogr., Kristallgeom., Kristallphys., Kristallchem.*, 1976, **143**, 14.
19 K. R. Swanson and J. J. Spijkerman, *J. App. Phys.*, 1970, **41**, 3155.
20 E. Murad and J. H. Johnston, in *Mössbauer Spectroscopy Applied to Inorganic Chemistry*, ed. G. J. Long, Plenum, New York, London, 1987, vol. 2, p. 523.
21 F. Izumi, *J. Solid State Chem.*, 1981, **38**, 381.
22 P. A. Flinn, in *Mössbauer Isomer Shifts*, eds. G. K. Shenoy and F. E. Wagner, North Holland, Amsterdam, 1978, p. 606.

*Received* 18*th January* 1994; *Paper* 4/00318G